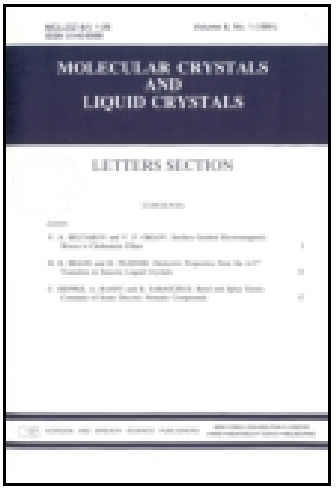

Molecular Crystals and Liquid Crystals
Publication details, including instructions for authors and subscription information:
http://www.tandfonline.com/loi/gmcl20

FTIR Spectroscopy of Hydrogen-Bonded Cu(N-R-Salim)$_2$ Dye Complexes

K. J. Dodia[a] & A. T. Oza[a]
[a] Department of Physics, Sardar Patel University, Gujarat, India
Published online: 28 Apr 2014.

To cite this article: K. J. Dodia & A. T. Oza (2014) FTIR Spectroscopy of Hydrogen-Bonded Cu(N-R-Salim)$_2$ Dye Complexes, Molecular Crystals and Liquid Crystals, 592:1, 1-27, DOI: 10.1080/15421406.2013.837995

To link to this article: http://dx.doi.org/10.1080/15421406.2013.837995

Mol. Cryst. Liq. Cryst., Vol. 592: pp. 1–27, 2014

ISSN: 1542-1406 print/1563-5287 online
DOI: 10.1080/15421406.2013.837995

Taylor & Francis
Taylor & Francis Group

FTIR Spectroscopy of Hydrogen-Bonded Cu(N-R-Salim)$_2$ Dye Complexes

K. J. DODIA* AND A. T. OZA

Department of Physics, Sardar Patel University, Gujarat, India

Some of bis(N-R-salicylaldiminato)Cu^{II} where R = H, CH_3, C_2H_5, and C_6H_5 are found to have copper chains in one direction of the crystals. These 1-d systems are hydrogen bonded with six highly polarizable dyes namely Para red, Congo red, Direct red, Bismark brown, Evans blue, and Trypan blue. The Fourier transform infrared (FTIR) spectra reveal infrared absorption edge and its modification with exciton-phonon coupling. Threshold energies for the formation of excitons with phonon emissions are observed. When exciton-phonon coupling is weak, a large number of phonon bands are observed in the edge spectrum. Free excitons are strongly bound and bound excitons are weakly bound to phonons.

Keywords Absorption edge; exciton-phonon coupling; FTIR spectra; hydrogen bond; indirect transitions

Introduction

Infrared analogies of optical phenomena in soft semiconductors have been an interesting subject. These analogies included nature of transition [1–18] band tailing [9,10,12,13], free-carrier absorption [1,9,10,12–14,16], Franz-Keldysh or Redfield effect [9,10,12,13], Burstein-Moss shift, spin-orbit splitting of valence band [19], pairing of charge carriers [20], harmonic generation and heterodyning, two-dimensional absorption functions [21], correlated hopping [19,22], noise in photoconductors [8], and square-root singularity in one dimension [15]. Thus the optical phenomena mentioned above which appear in UV-visible range in inorganic compound semiconductors appear in infrared range in organic and metal-organic semiconductors. Here in the present work, exciton-phonon coupling which occurs in GaP [23–26], SiC [27], CdSe [28], AgBr [29,30], ZnO [31], GaAs [32], and carbon nanotubes [33] is observed in soft semiconductors such as hydrogen-bonded dyes with bis(N-R-salicylaldiminato)Cu^{II} metal organic l-d system hydrogen bonded with six dyes. The Urbach optical absorption edge is also studied in details [34].

Experimental Details

Bis(N-R-salicylaldiminato)Cu^{II} chelates where R = H, CH_3, C_2H_5, and C_6H_5 were prepared by reactions of nickel ion (ionic solutions of nickel chloride) with salicyldehyde and ammonia solution, methylamine, ethylamine, and aniline in the presence of a base. These

*Address correspondence to K. J. Dodia, Department of Physics, Sardar Patel University, Vallabh Vidyanagar 388120, Gujarat, India. E-mail: ketanjdodia@gmail.com

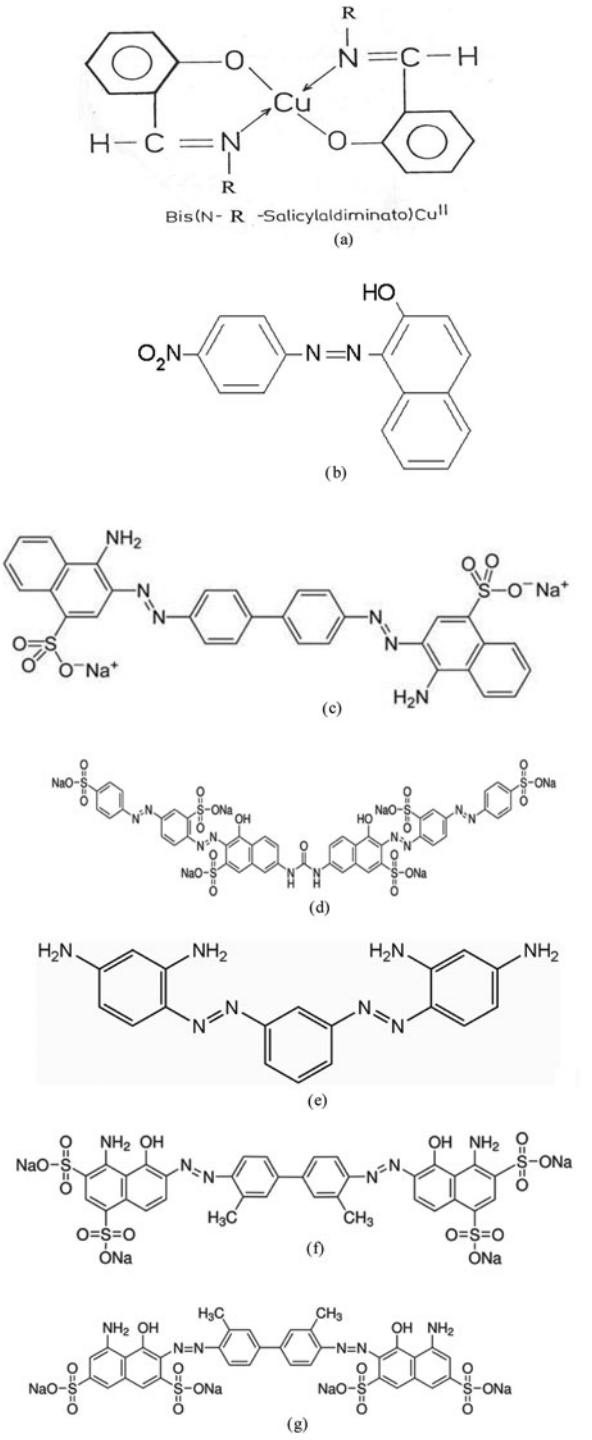

Figure 1. (a) Molecular structures of Cu(N-R-salim)2 where R = H, CH_3, C_2H_5, and C_6H_5, (b) Para red, (c) Congo red, (d) Direct red, (e) Bismark brown, (f) Evans blue, and (g) Trypan blue.

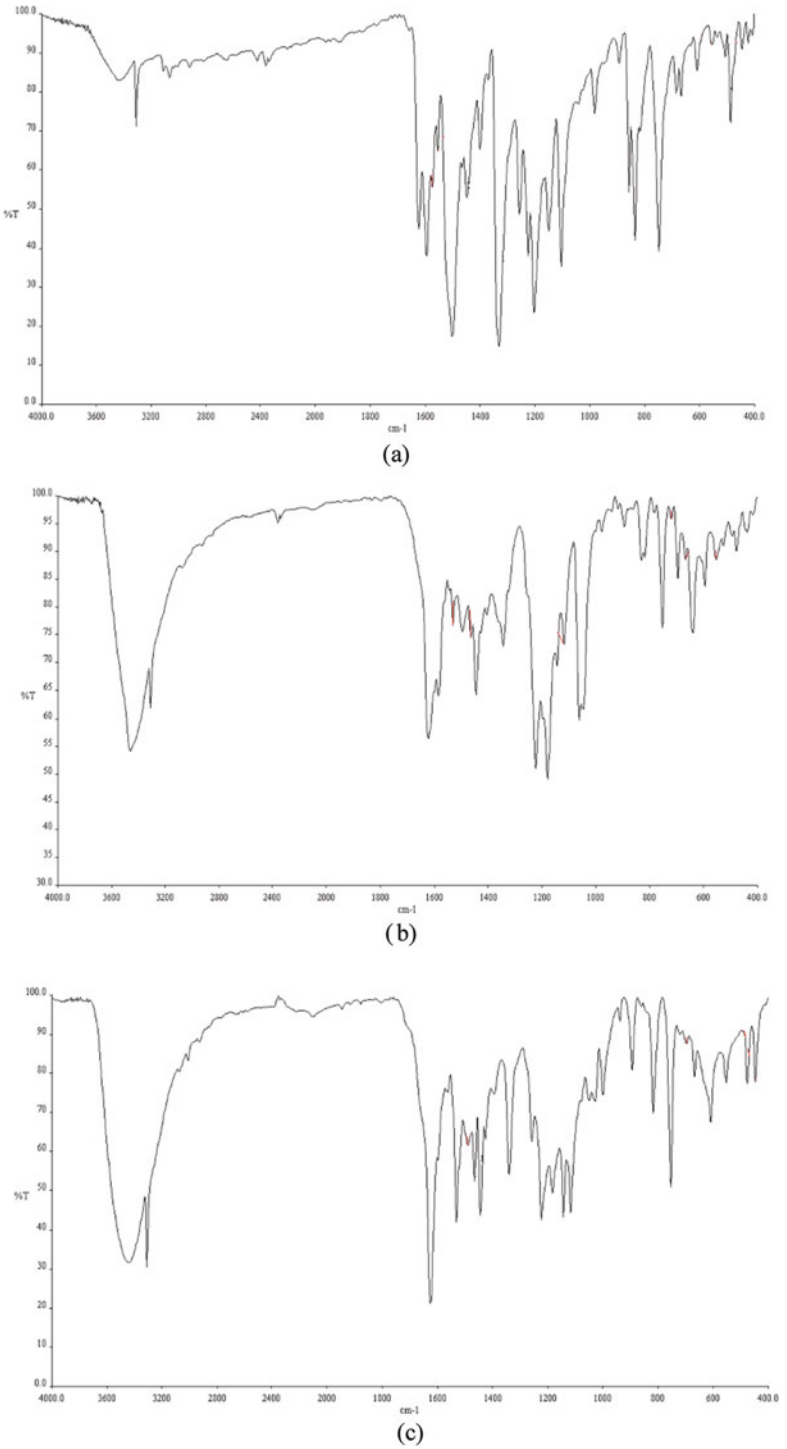

Figure 2. FTIR spectra of complexes of Cu(N-H-salim)$_2$ with (a) Para red, (b) Congo red, (c) Direct red, (d) Bismark brown, (e) Evans blue, and (f) Trypan blue. *(Continued)*

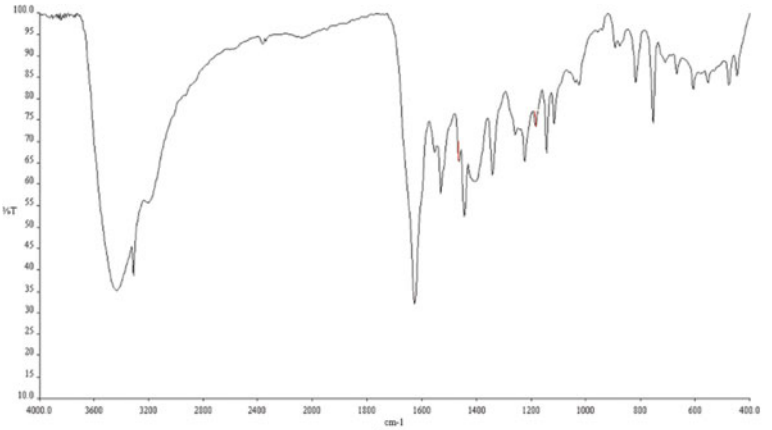

(d)

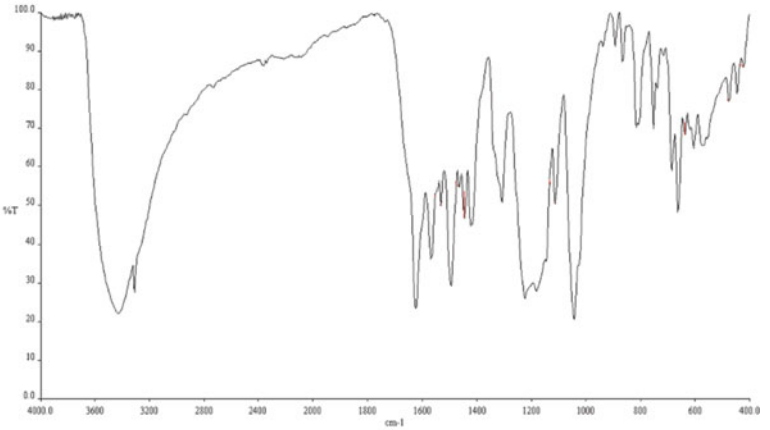

(e)

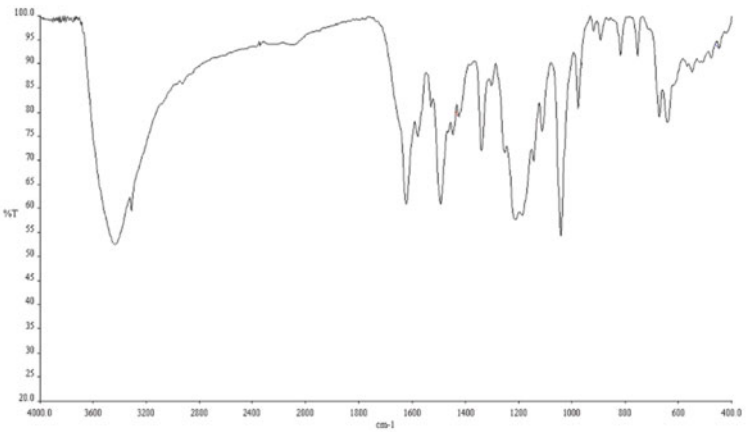

(f)

Figure 2. (Continued).

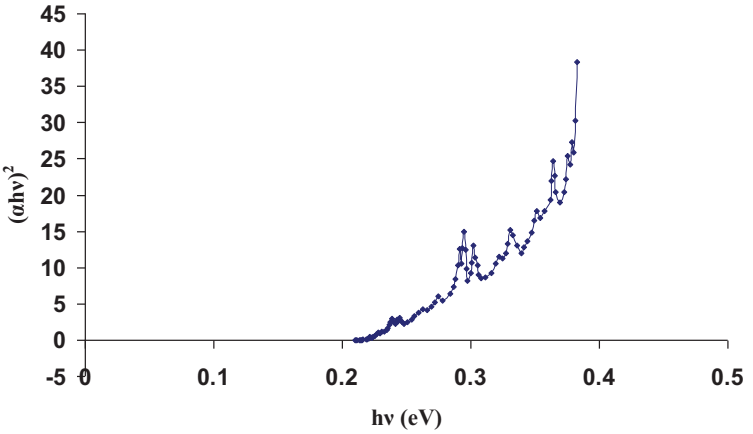

(a)

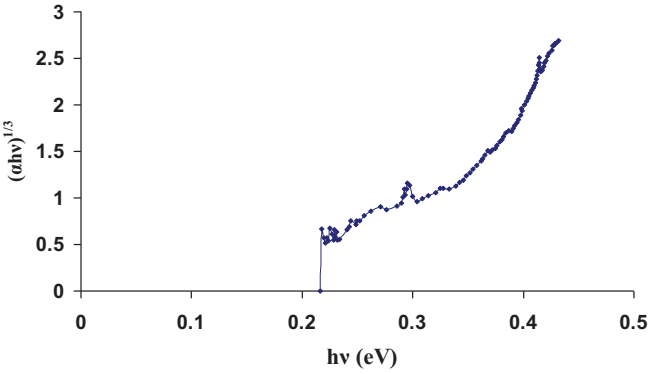

(b)

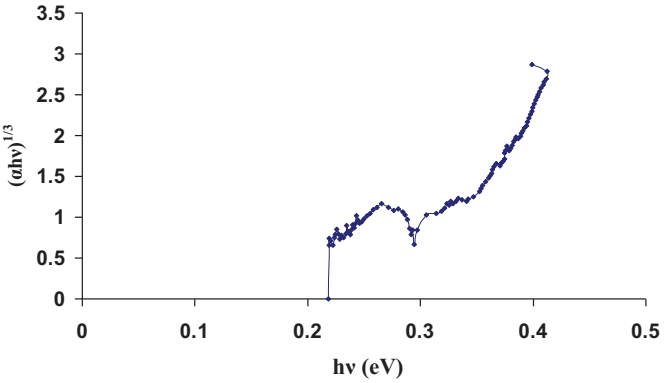

(c)

Figure 3. Nature of transitions in complexes of Cu(N-H-salim)$_2$ with (a) Para red, (b) Congo red, (c) Direct red, (d) Bismark brown, (e) Evans blue, and (f) Trypan blue. *(Continued)*

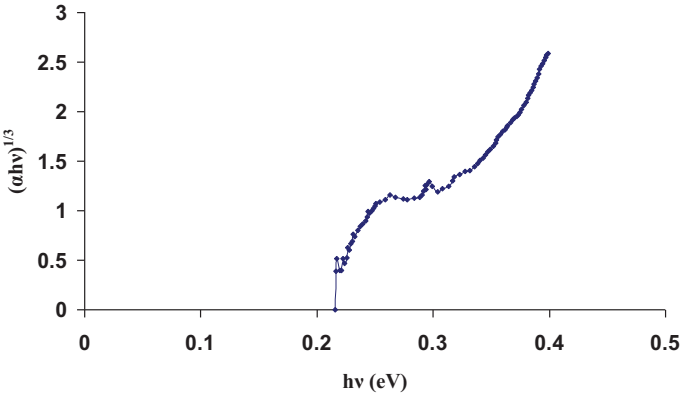

(d)

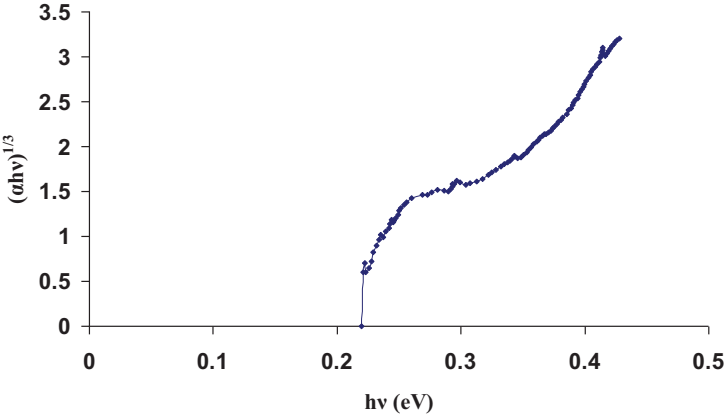

(e)

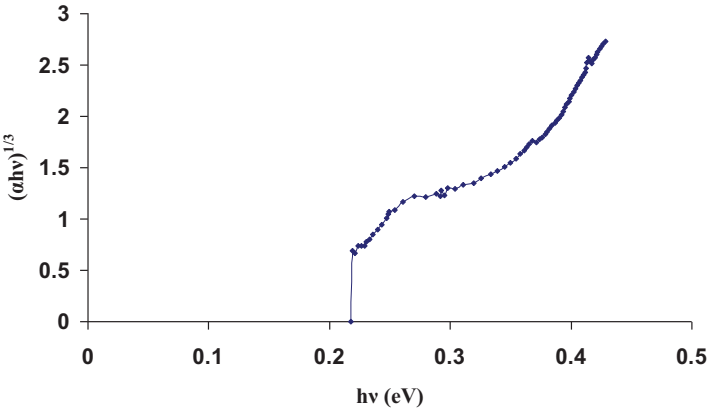

(f)

Figure 3. (Continued)

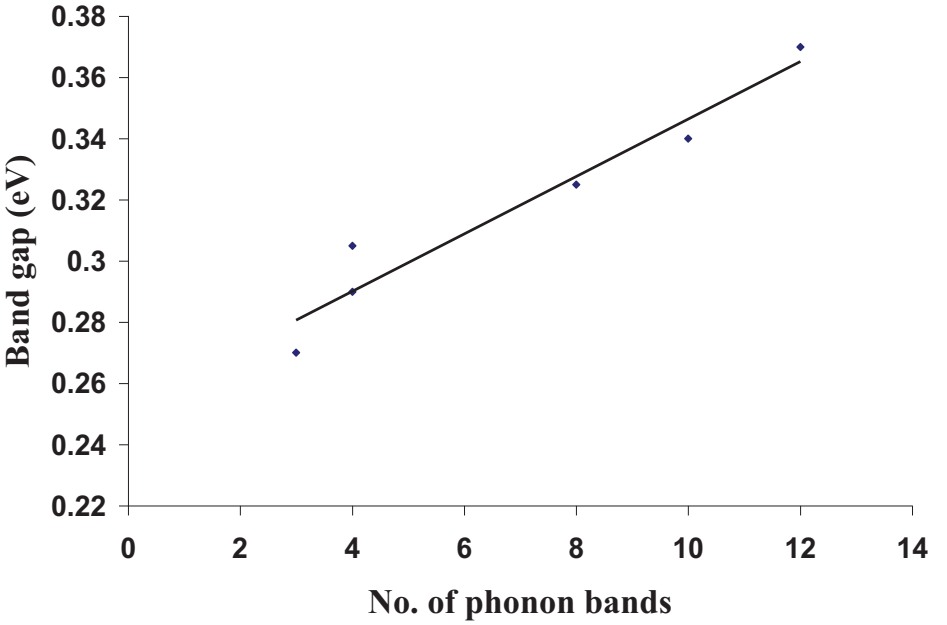

Figure 4. The number of phonon bands vs. band gap for Cu(N-H-salim)$_2$ complexes.

green colored chelates were mixed and grinded with six dyes, namely Para red, Congo red, Direct red, Bismark brown, Evans blue, and Trypan blue obtained in pure forms from Aldrich chemical company. The fine and homogeneous powders prepared in this manner were remixed with dry (anhydrous) spectrograde KBr powder in 95% amount and grinded. The semitransparent pallets were prepared by compressing these mixtures in a circular die with the help of a manually operated compressing machine. Then these circular discs were placed in a dark chamber of a spectrophotometer.

The spectra in the range 400–4000 cm^{-1} were recorded using a GXFTIR single beam spectrophotometer manufactured by Perking-Elmer Co., USA. It was having a resolution of 0.15 cm^{-1}, a scan range of 15,600-30 cm^{-1}, a scan time of 20 scan sec^{-1}, an OPD velocity of 0.20 cm sec^{-1}, and MIRTGS and FIRTGS detectors. A bean splitter of opt-KBr type was used having a range of 7800-370 cm^{-1}. The spectra were recorded in purge mode.

Result and Discussion

The molecular structures of bis(N-R-salicylaldiminato)Cu^{II} where R = H, CH_3, C_2H_5, and C_6H_5 and six dyes are shown (Figure 1). The dyes show hydrogen bondings of N—H—O type, O—H—O type, N—H—π type and O—H—π type between the dyes and the copper chelates. Hydrogen bonding is confirmed with Fourier transform infrared (FTIR) spectroscopy. $N^{\delta+}$**-H—O**$^{\delta-}$, **O**$^{\delta+}$**-H—O**$^{\delta-}$, $N^{\delta+}$**-H—**$\pi^{\delta-}$, and $O^{\delta+}$**-H—**$\pi^{\delta-}$ type bonding lead to excitons due to $\delta+$ and $\delta-$ charges. There are no free electronic excitations in either copper chelates or the six dyes. The electronic excitations are found in hydrogen-bonded complexes only. Thus excitons and hydrogen bonds are related. Highly polarized dyes work as side chains across which electronic oscillations occur and molecular excitons are formed. For long side chains, these molecular excitons nearly act as Mott-Wannier excitons, which are weakly bound. Molecular dipoles oscillate as the long-chain dye molecules have dipole

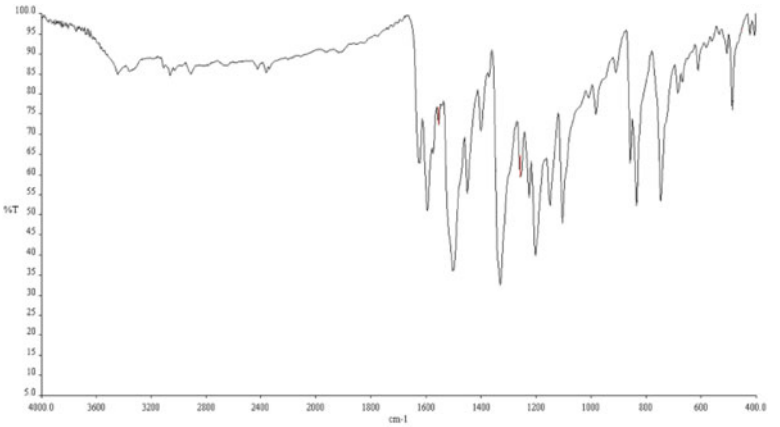

(a)

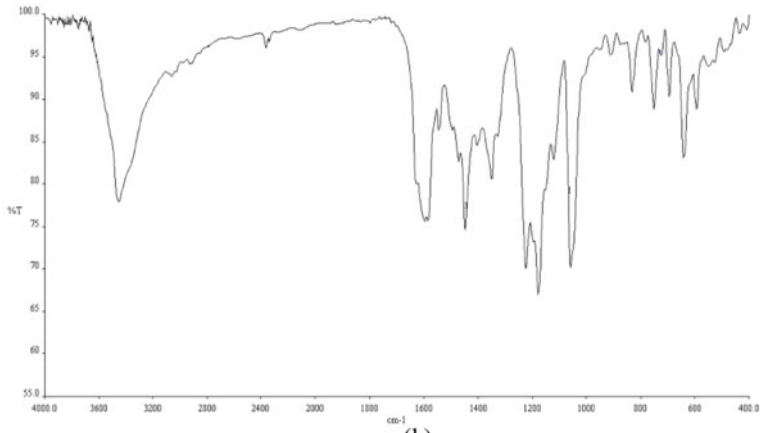

(b)

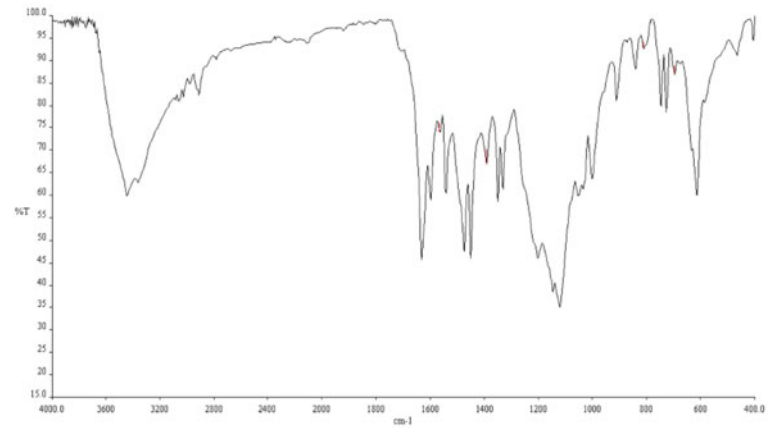

(c)

Figure 5. FTIR spectra of the complexes of Cu(N-CH_3-salim)$_2$ with (a) Para red, (b) Congo red, (c) Direct red, (d) Bismark brown, (e) Evans blue, and (f) Trypan blue. *(Continued)*

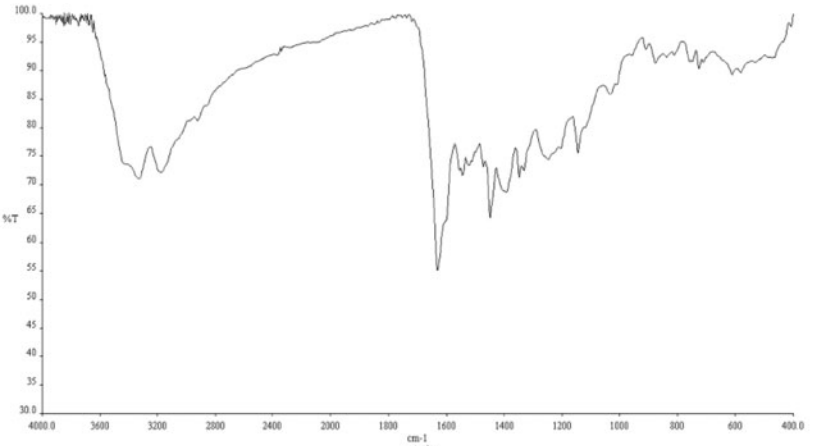

(d)

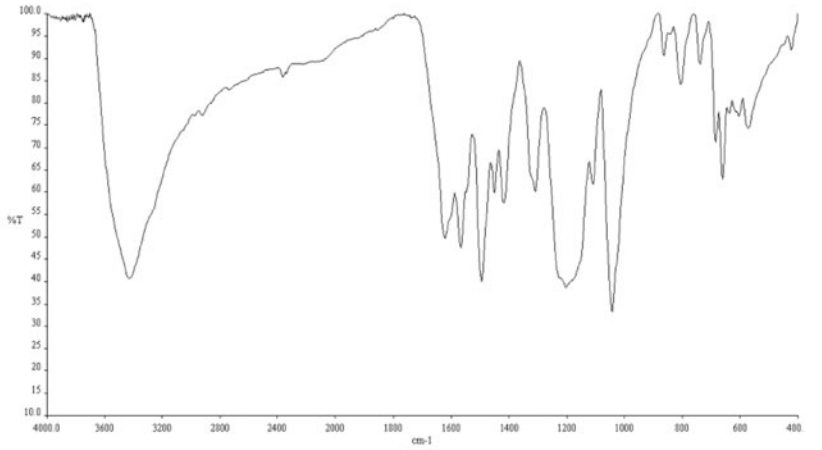

(e)

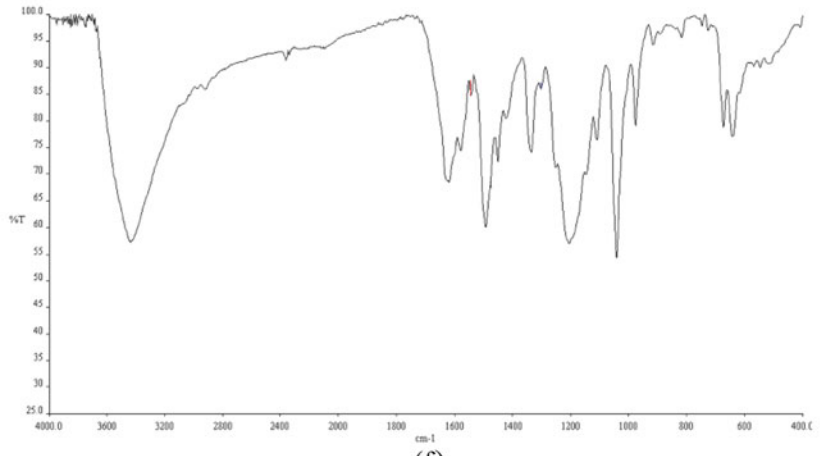

(f)

Figure 5. (Continued)

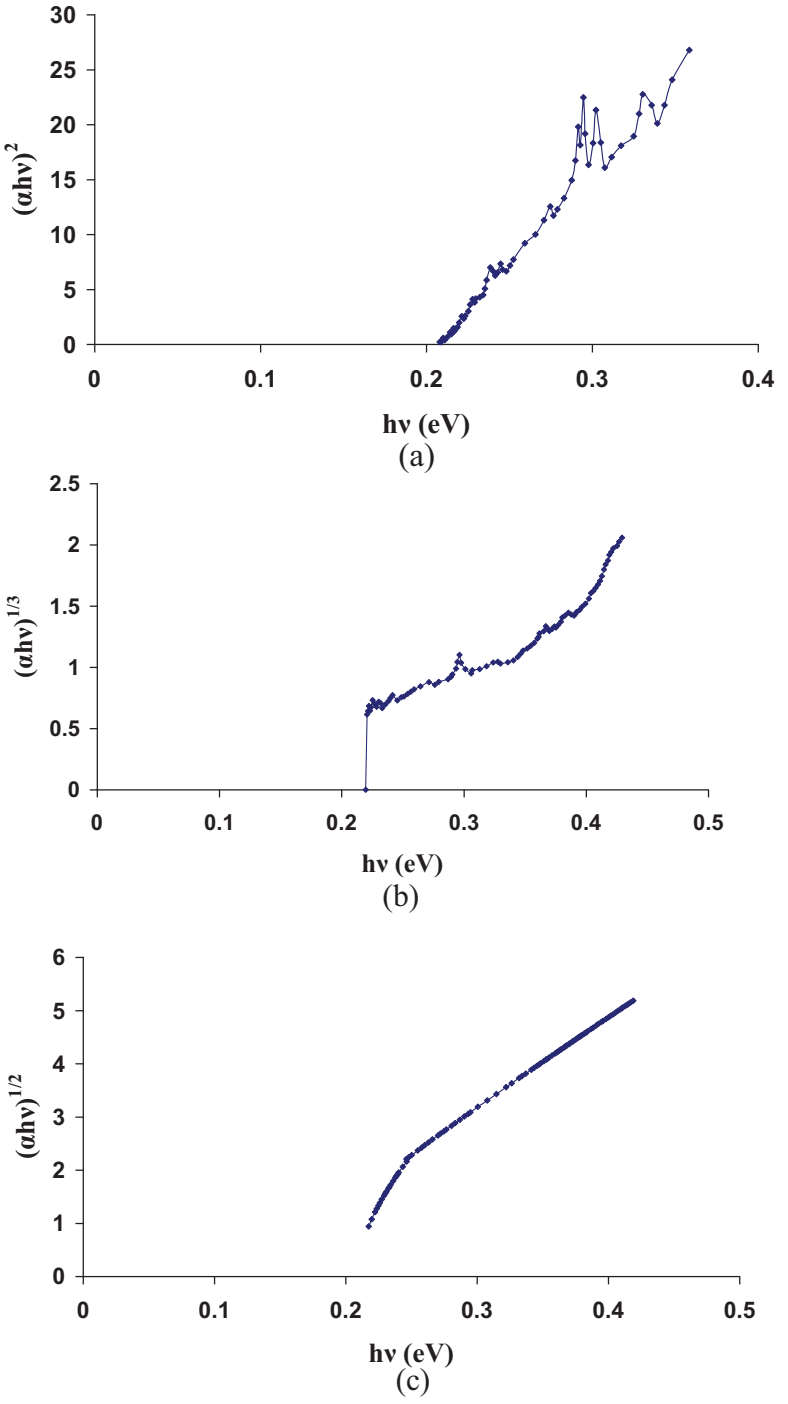

Figure 6. Nature of transitions in the complexes of $Cu(N\text{-}CH_3\text{-}salim)_2$ with (a) Para red, (b) Congo red, (c) Direct red, (d) Bismark brown, (e) Evans blue, and (f) Trypan blue. *(Continued)*

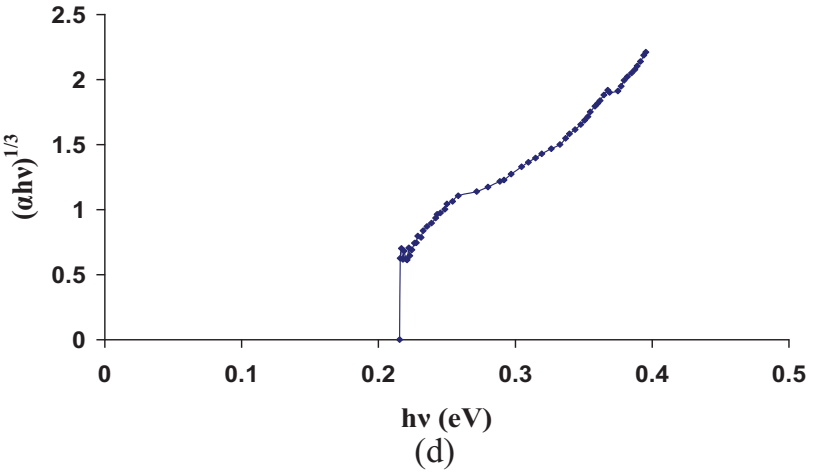

(d)

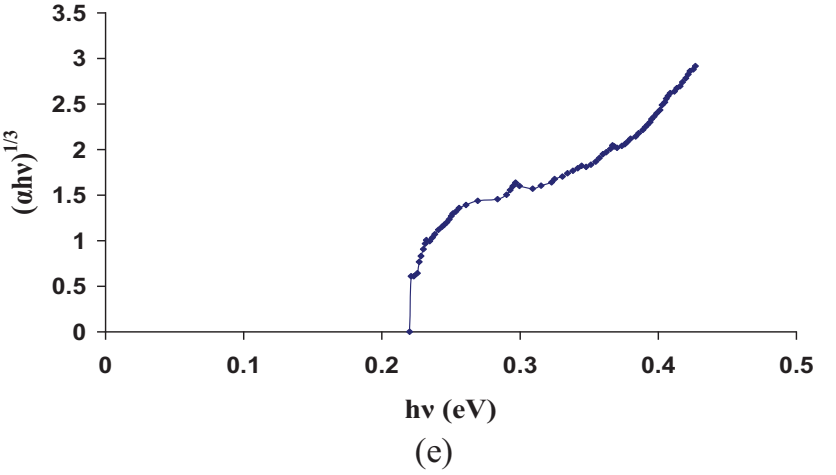

(e)

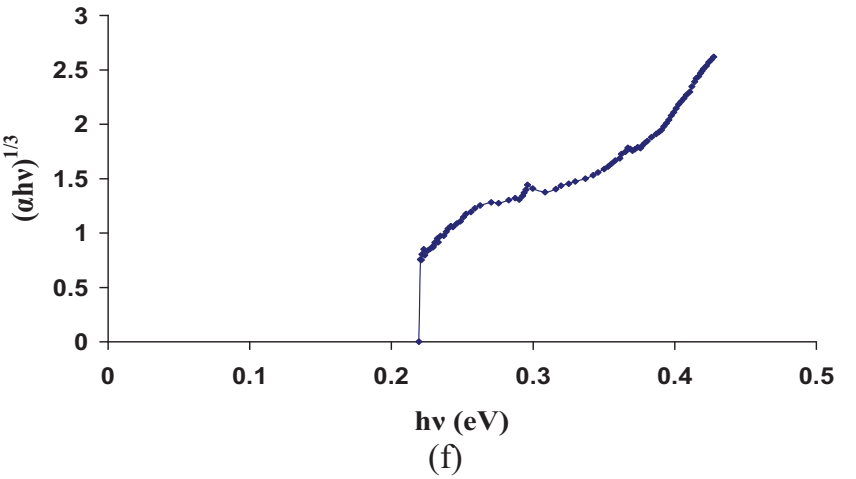

(f)

Figure 6. (Continued)

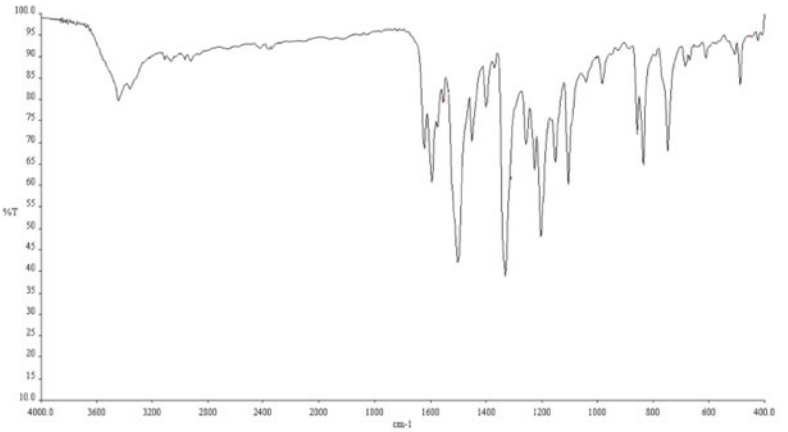

(a)

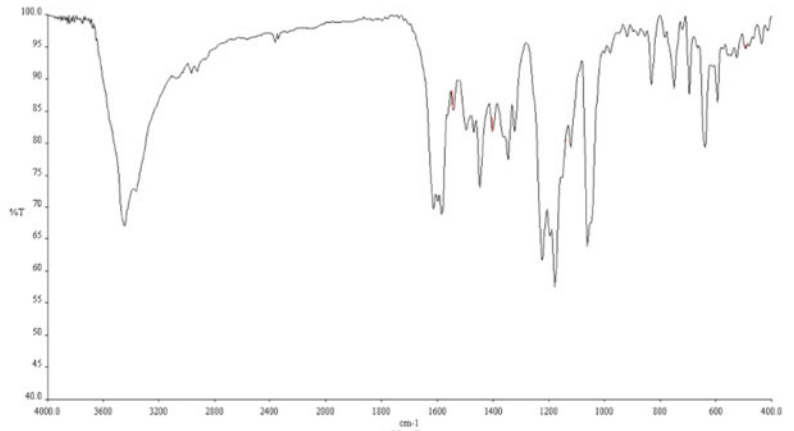

(b)

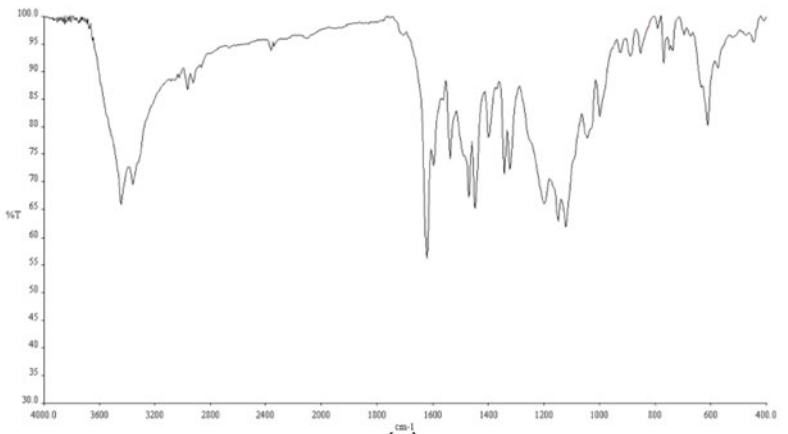

(c)

Figure 7. The number of phonon bands vs. band gap for Cu(N-CH_3- salim)$_2$ complexes. *(Continued)*

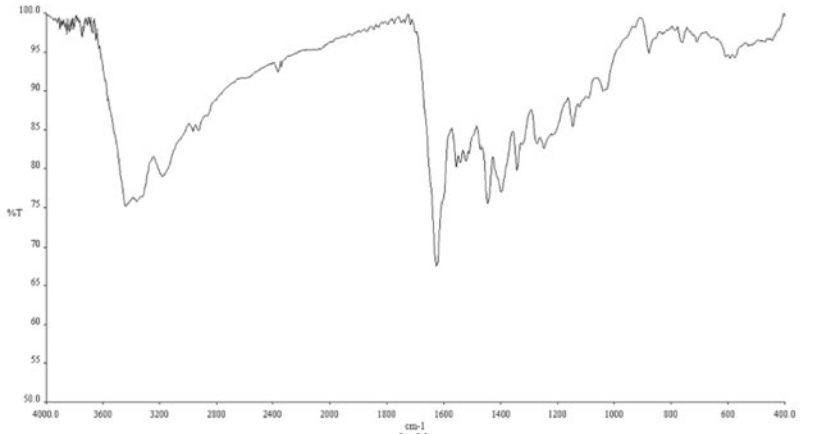

(d)

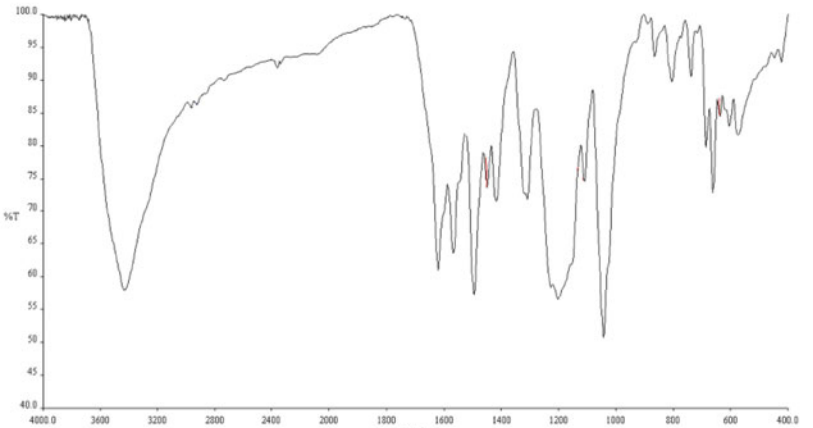

(e)

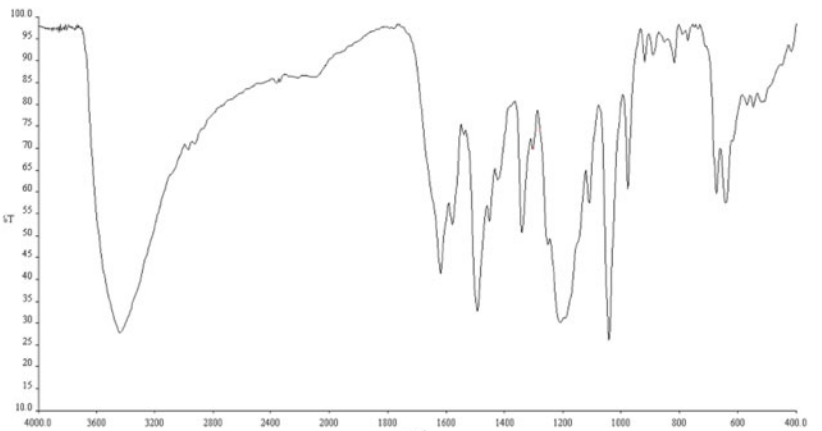

(f)

Figure 7. (Continued)

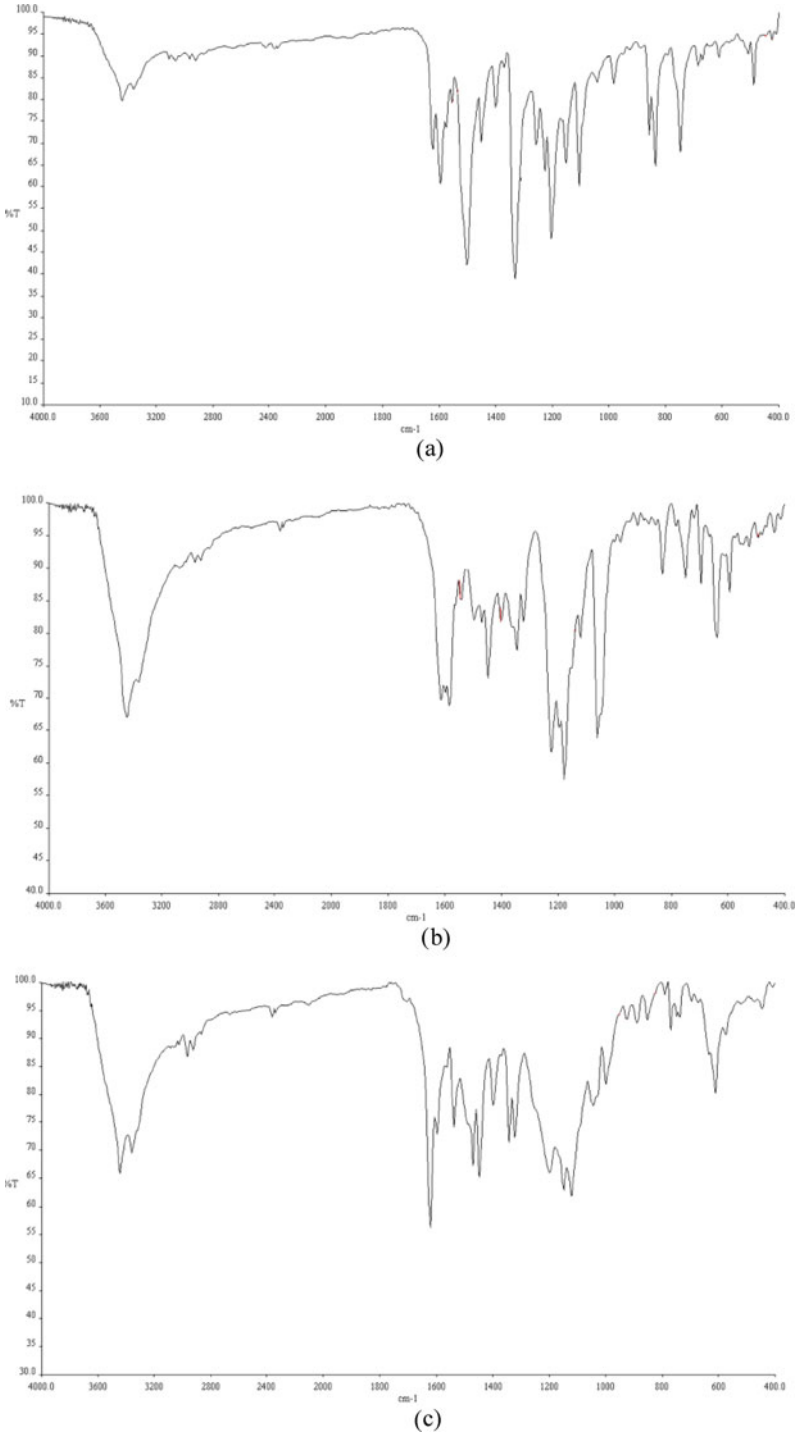

Figure 8. FTIR spectra of the complexes of $Cu(N\text{-}C_2H_5\text{-salim})_2$ with (a) Par red, (b) Congo red, (c) Direct red, (d) Bismark brown, (e) Evans blue, and (f) Trypan blue. *(Continued)*

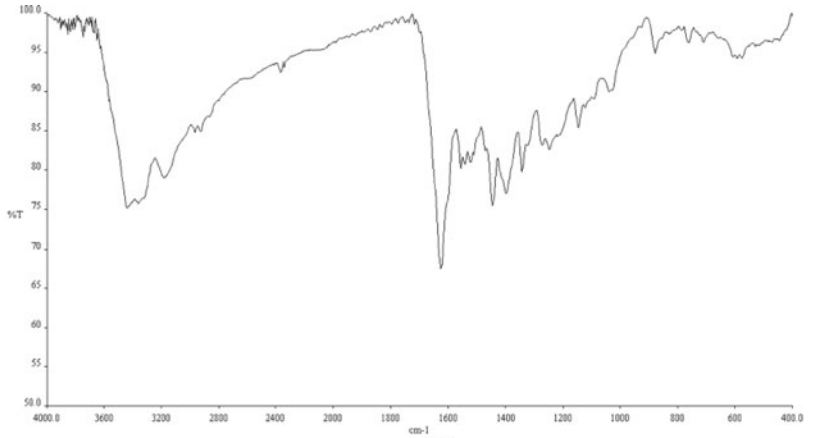

(d)

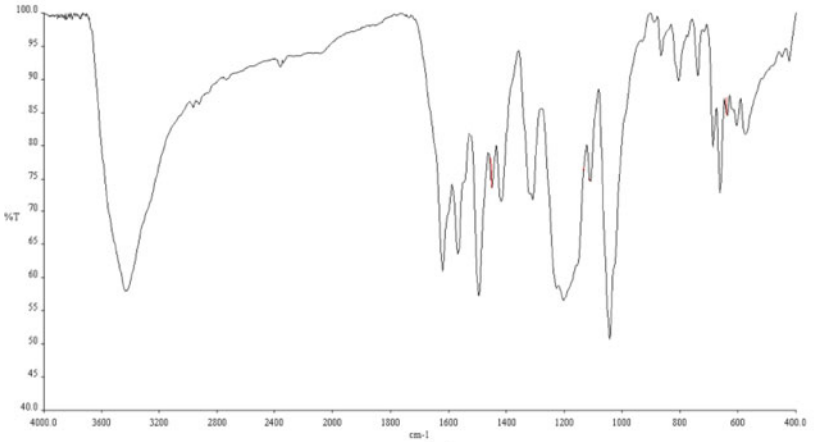

(e)

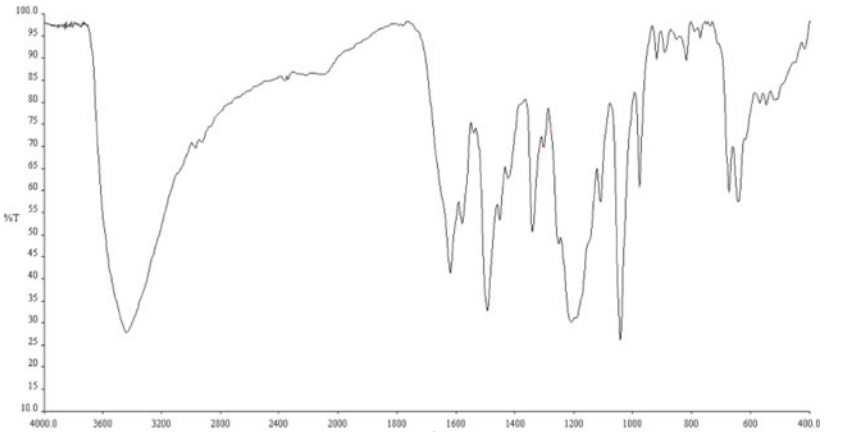

(f)

Figure 8. (Continued)

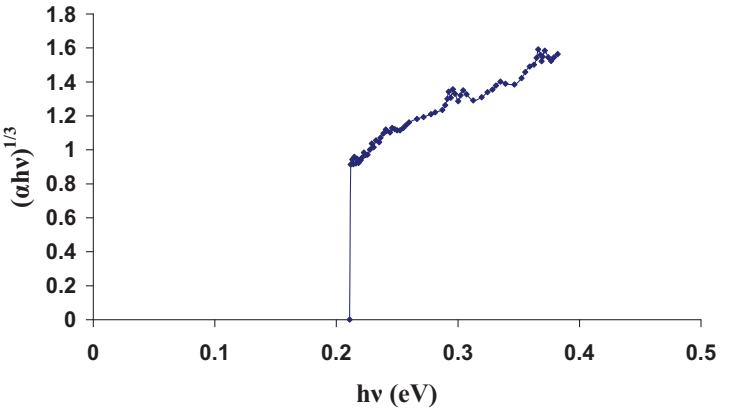

(a)

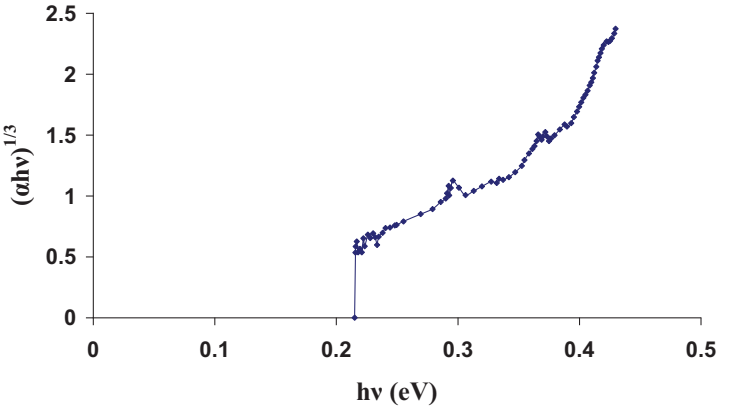

(b)

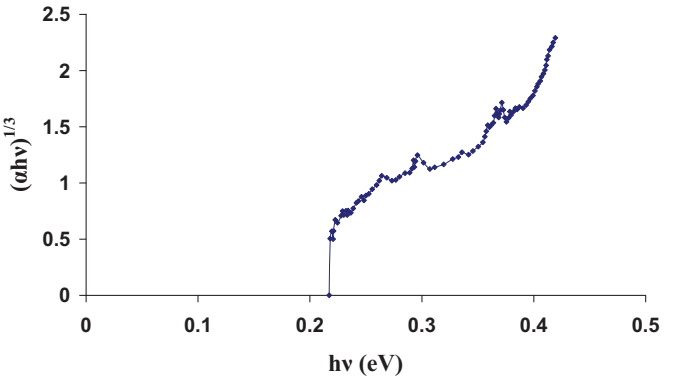

(c)

Figure 9. Nature of transitions in the complexes of $Cu(N\text{-}C_2H_5\text{-}salim)_2$ with (a) Para red, (b) Congo red, (c) Direct red, (d) Bismark brown, (e) Evans blue, and (f) Trypan blue. *(Continued)*

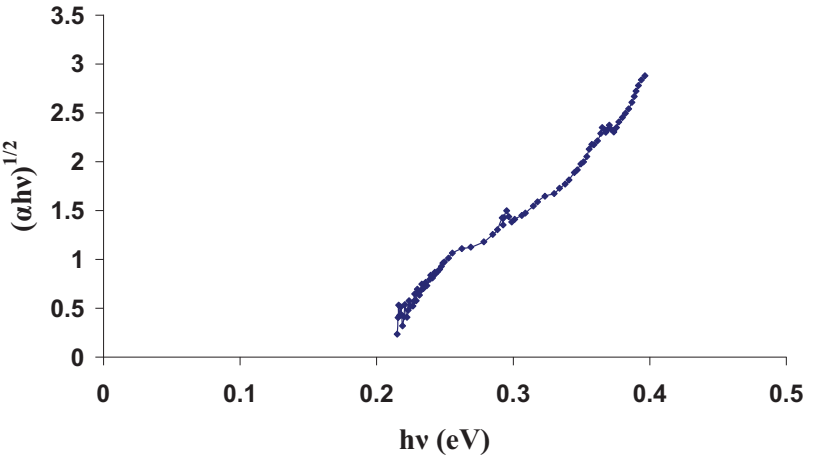

(d)

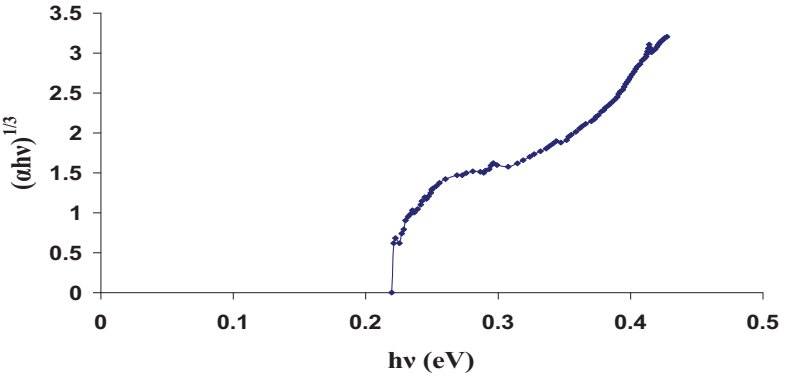

(e)

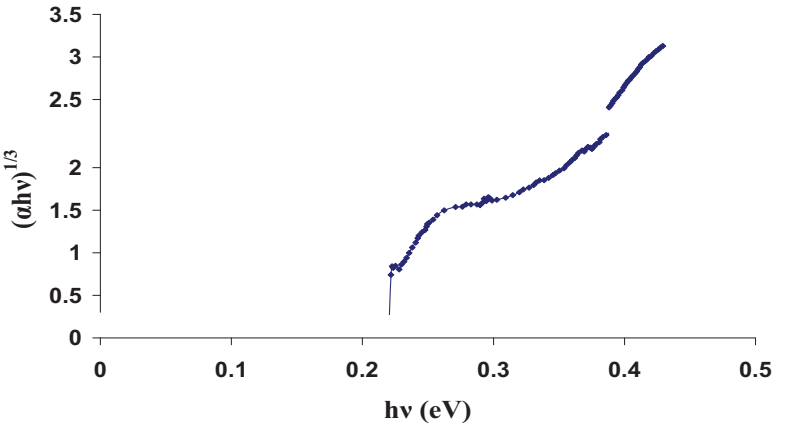

(f)

Figure 9. (Continued)

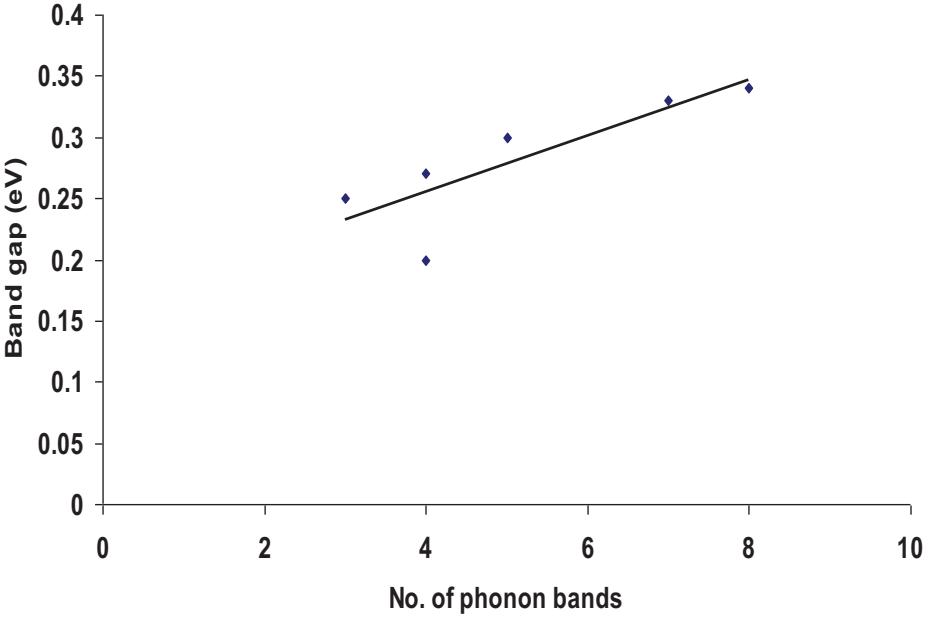

Figure 10. The number of phonon bands vs. band gap for Cu(N-C_2H_5-salim)$_2$ complexes.

moments of several debyes. Dipole flip-flop continues without any hindrance. Induced charge appearing along copper chelate molecules moves across the metal chain which acts as a spine.

The FTIR spectra of Cu^{II}(N-H-salim)$_2$ bonded with six dyes namely Para red, Congo red, Direct red, Bismark brown, Evans blue, and Trypan blue are shown (Figure 2). The natures of transitions are fitted and best fits are shown (Figure 3). Cu(N-H-salim)$_2$-Para red shows direct transition by fitting $\alpha h\nu = A(h\nu - E_g)^{1/2}$ [i.e., $(\alpha h\nu)^{1/2}$ vs. $h\nu$]. All other complexes show forbidden indirect transition obeying $\alpha h\nu = A(h\nu - E_g)^3$ [i.e., $(\alpha h\nu)^{1/3}$ vs. $h\nu$]. The number of phonon bands vs. band gap is plotted and almost shows a linear variation (Figure 4). When the exciton-phonon coupling is weak, more numbers of phonons are emitted and there are also more numbers of threshold energies of excitons. The band gap is large in this case. When exciton-phonon coupling is strong, there are less numbers of phonon emission bands and band gap is small. In the former case, the exciton density is high and there is more probability for the formation of electron-hole droplets particularly at low temperatures. In the latter case when band gap is small, there is more probability of recombinations of electron-hole pairs and consequently more possibility of infrared luminescence.

The FTIR spectra of Cu(N-CH_3-salim)$_2$ bonded with six dyes are also shown (Figure 5). Cu(N-CH_3-salim)$_2$-Para red shows allowed direct transition, Congo red complex shows forbidden indirect transition, Direct red complex shows allowed indirect transition, and Bismark brown, Evans blue, and Trypan blue complex shows forbidden indirect transitions, the best fits are shown (Figure 6). The number of phonon bands vs. band gap is plotted (Figure 7), which again shows a rectilinear behavior. The numbers of phonon bands are less for the same dye than those found for Cu(N-H-salim)$_2$ chelate. This shows that the

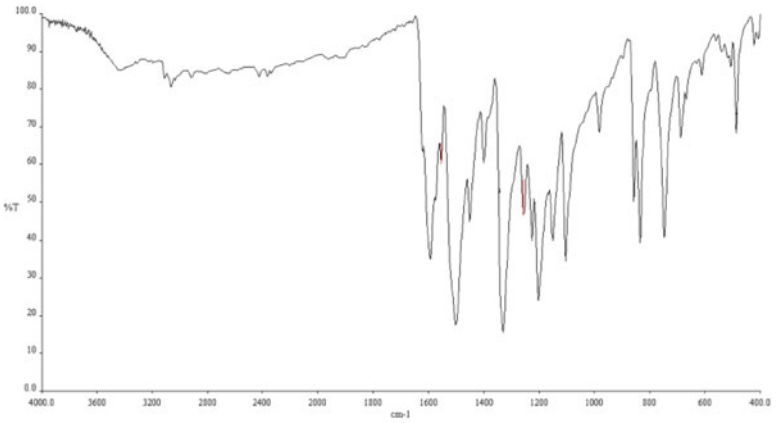

(a)

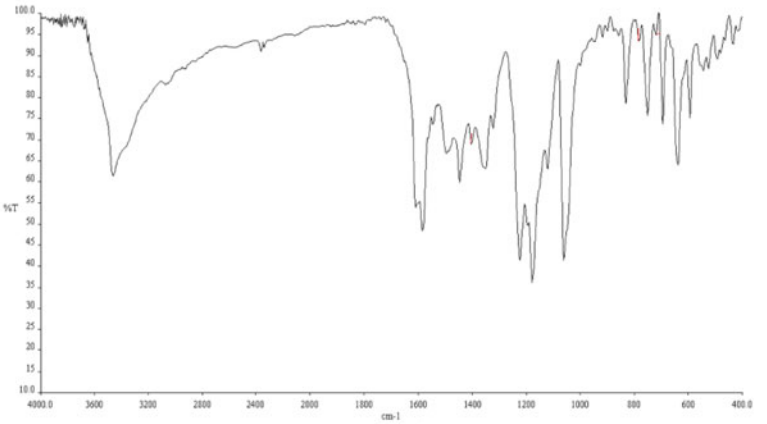

(b)

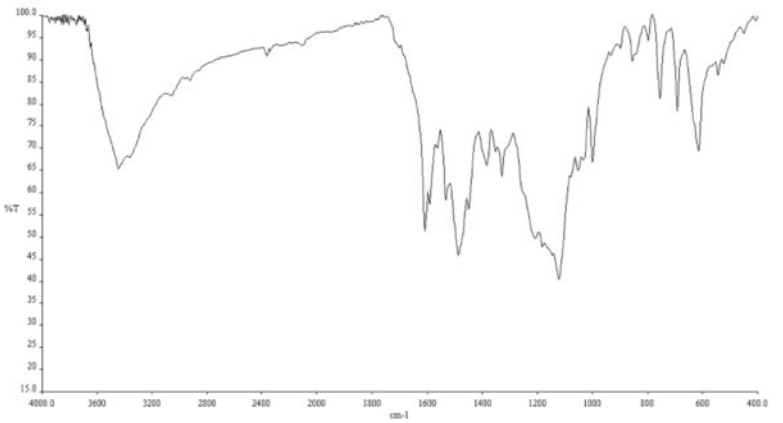

(c)

Figure 11. FTIR spectra of the complexes of $Cu(N\text{-}C_6H_5\text{-}salim)_2$ with (a) Par red, (b) Congo red, (c) Direct red, (d) Bismark brown, (e) Evans blue, and (f) Trypan blue. *(Continued)*

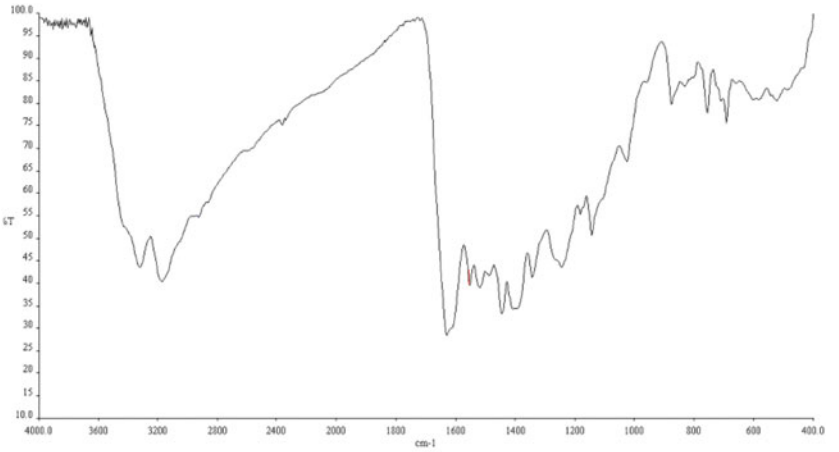

(d)

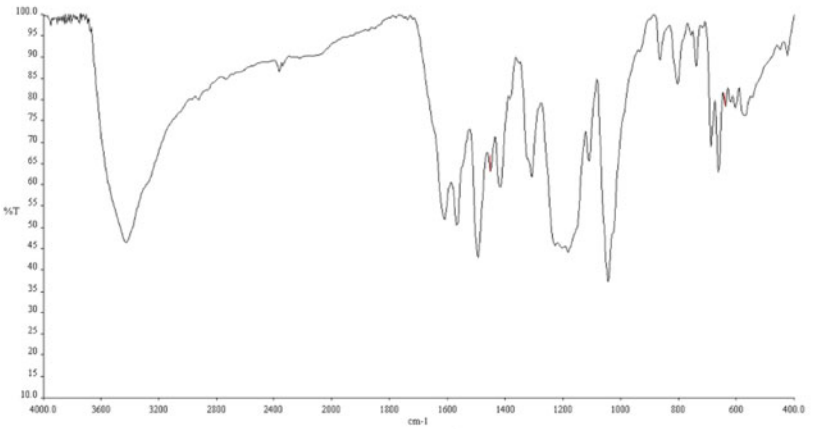

(e)

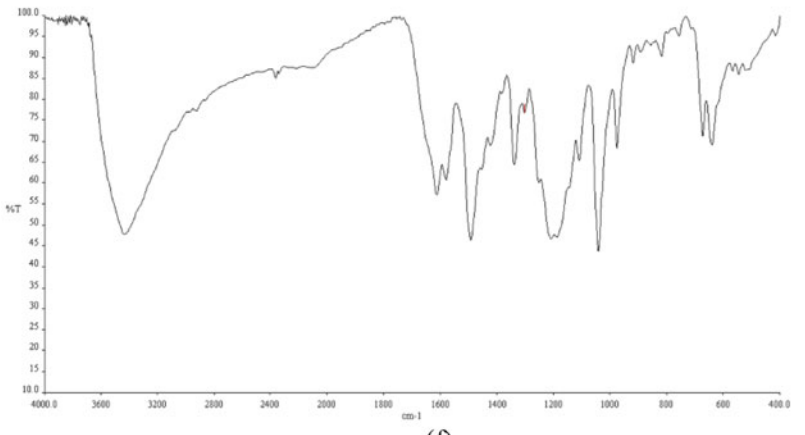

(f)

Figure 11. (Continued)

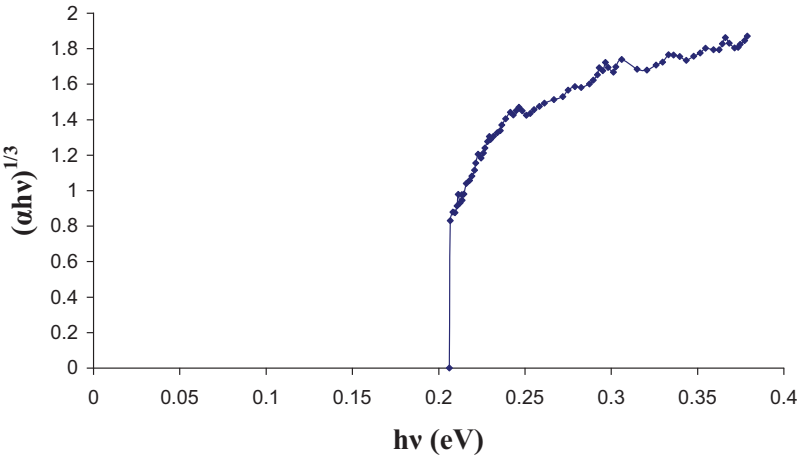

(a)

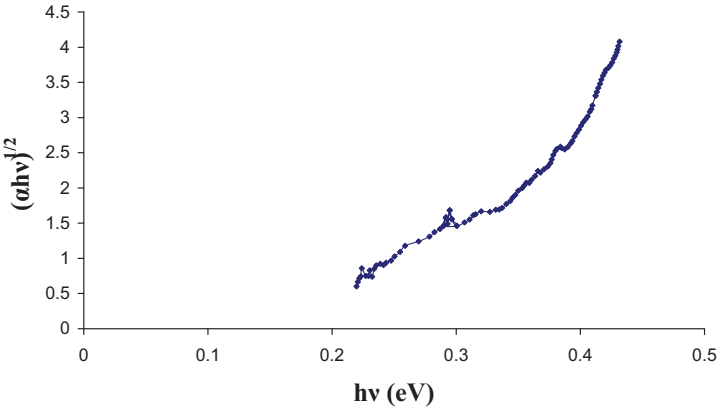

(b)

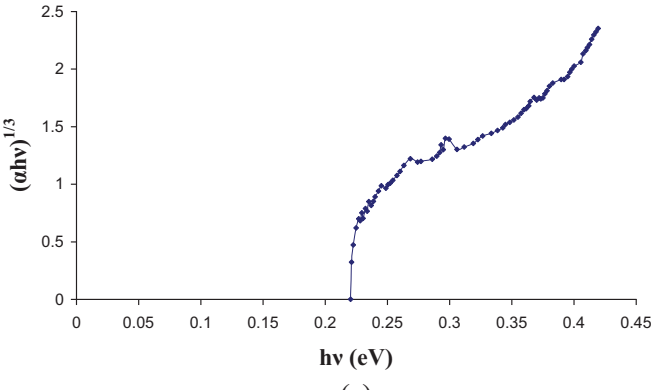

(c)

Figure 12. Nature of transitions in the complexes of $Cu(N\text{-}C_6H_5\text{-}salim)_2$ with (a) Para red, (b) Congo red, (c) Direct red, (d) Bismark brown, (e) Evans blue, and (f) Trypan blue. *(Continued)*

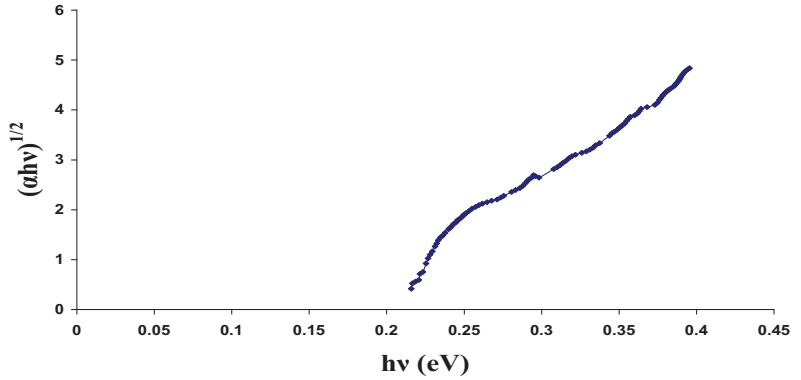

(d)

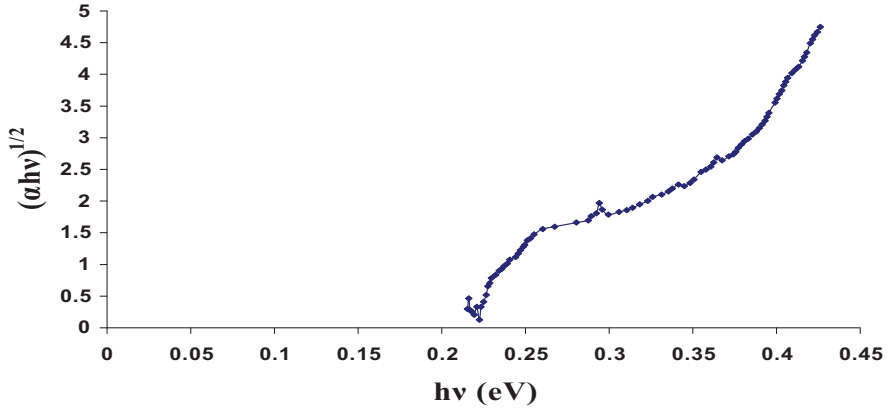

(e)

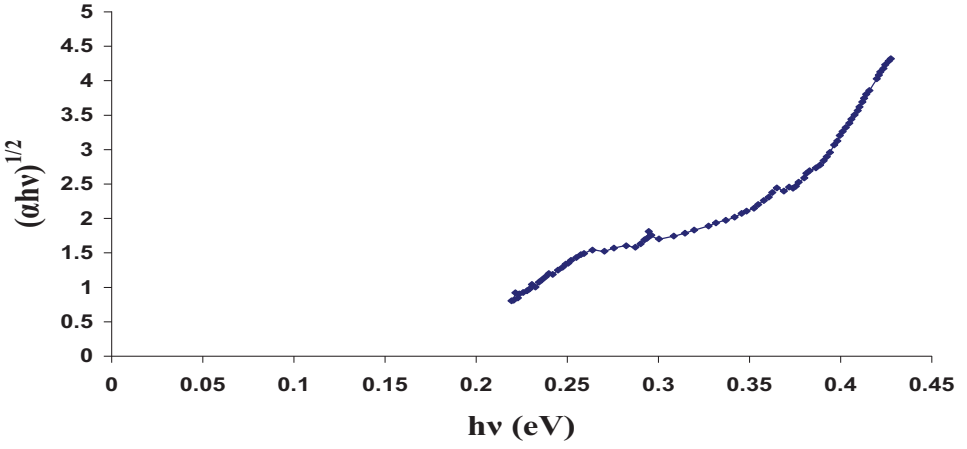

(f)

Figure 12. (Continued)

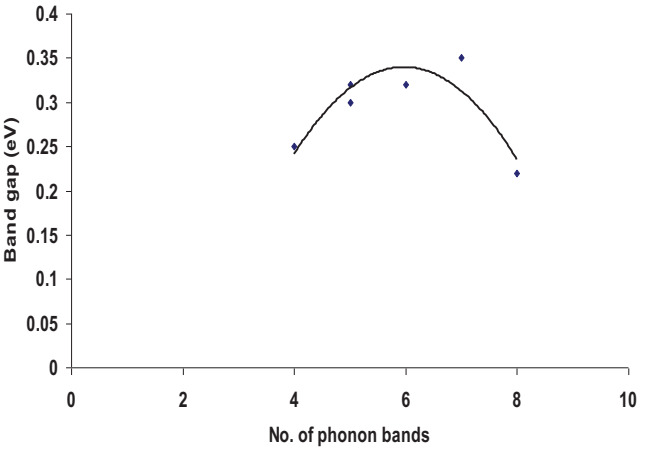

Figure 13. The number of phonon bands vs. band gap for Cu(N-C_6H_5-salim)$_2$ complexes.

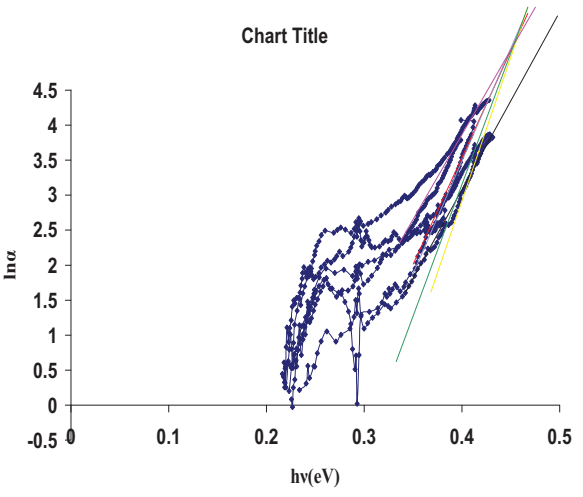

(a)

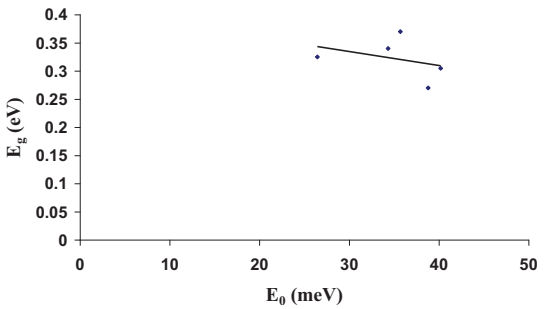

(b)

Figure 14. (a) Band tailing and focal point analysis for Cu(N-H-salim)$_2$ with six dyes, (b) E_g vs. E_0, i.e., band gap vs. width of the tail.

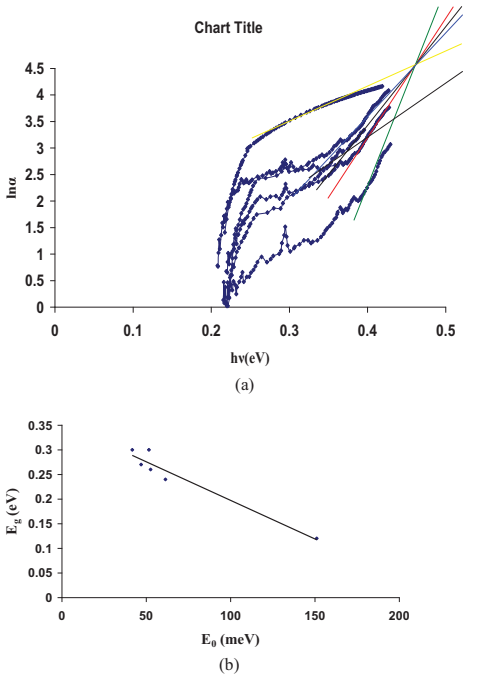

Figure 15. (a) Band tailing and focal point analysis for Cu(N-CH_3- salim)$_2$ with six dyes, (b) E_g vs. E_0, i.e., band gap vs. width of the tail.

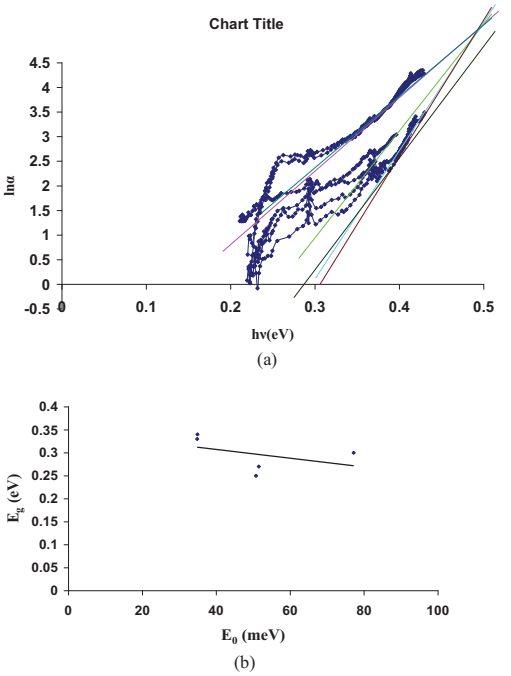

Figure 16. (a) Band tailing and focal point analysis for Cu(N-C_2H_5- salim)$_2$ with six dyes, (b) E_g vs. E_0, i.e., band gap vs. width of the tail.

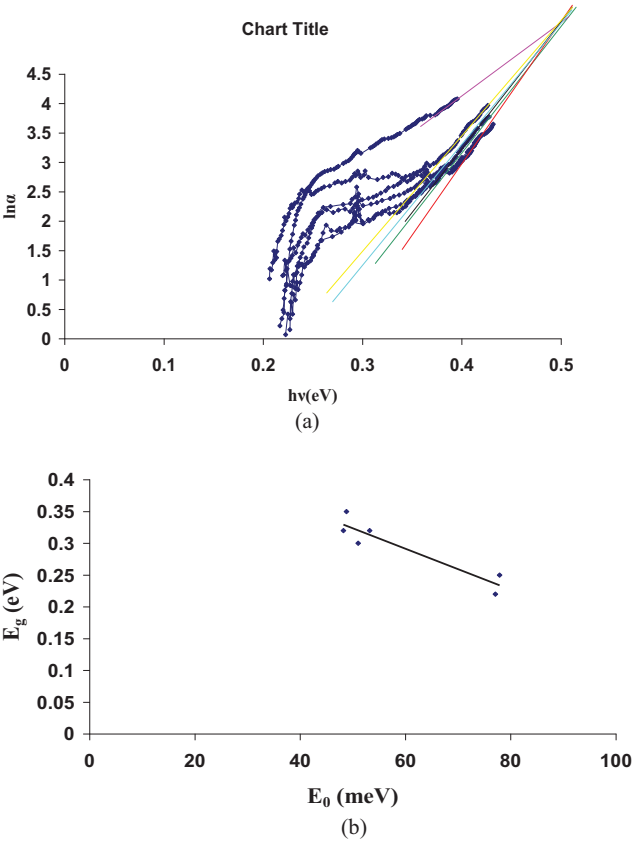

Figure 17. (a) Band tailing and focal point analysis for Cu(N-C_6H_5-salim)$_2$ with six dyes, (b) E_g vs. E_0, i.e., band gap vs. width of the tail.

exciton-phonon coupling is stronger for Cu(N-CH_3-salim)$_2$ chelate than that for Cu(N-H-salim)$_2$ chelate. The Direct red complex shows strongest exciton-phonon coupling with zero number of phonon bands and behavior similar to those found in hydrogen-bonded inclusion compounds of iodine. In this case, band gap as low as 0.12 eV is found. Exciton energy of 0.08 eV (80 eV) is noted because of Tauc energy gap $E_g = 0.2$ eV.

The FTIR spectra of Cu(N-C_2H_5-salim)$_2$ hydrogen bonded with the above mentioned six dyes are shown (Figure 8). Natures of transitions are fitted and best fits are shown (Figure 9). The number of phonon bands vs. band gap shows a straight line (Figure 10). The exciton-phonon coupling is strong, so band gap decreases as number of phonon band decreases.

The FTIR spectra of Cu(N-C_6H_5-salim)$_2$ hydrogen bonded with six dyes are also shown (Figure 11). Natures of transitions are analyzed and best fits are shown (Figure 12). The number of phonon band vs. gap again shows a curve for bulky ligand with benzene rings as a substitution (Figure 13). There is a plateau in band gap for large number of phonon bands. However the total number of phonon bands is not very high, indicating sufficient strength of exciton-phonon coupling. This shows more free excitons which are strongly bound to phonons. Cu(N-C_6H_5-salim)$_2$-Para red complex, in spite of having large number of phonon bands, has a very small band gap of only 0.16 eV. This does not fall anywhere on

the number of phonon bands vs. band gap curve and it is an exceptional case. About 10–12 phonon bands are found with weak but band gap is very small. In fact it shows excitonic binding energy almost equal to band gap with the behavior similar to the hydrogen-bonded inclusion compounds of iodine. Exciton emission occurs first and absorption is a secondary process. Thus an inverted behavior with respect to phonon emission and absorption is found. Emission threshold is lower than absorption threshold.

Band tailing of either a conduction band or a valence band or both is described by

$$\alpha = \alpha_0 \ \exp\{(h\nu - E_1)/E_0\} \tag{1}$$

where E_0 is called the width of the tail and E_1 is called the focal point. E_0 is a measure of amount of disorder and E_1 is the characteristic of the parent material. When E_0 is large, disorder is more. When $E_0 = k_B T$ it is called Urbach tail. E_0 is found as inverse of the slope of $\ln \alpha$ vs. $h\nu$ plot, because

$$E_0 = [\delta \ \ln \alpha / \delta(h\nu)]^{-1} \tag{2}$$

$$= 1/\text{slope} \tag{3}$$

This analysis is done here for Cu(N-R-salim)2 with six dyes for R = H, CH_3, C_2H_5, and C_6H_5 (Figures 14–17). The Tauc energy gap E_T found from plots of $(\alpha h\nu)^{1/r}$ vs. $h\nu$ and the width of tail E_0 as calculated from slope are plotted (Figures 14(b), 15(b), 16(b), 17(b)). It is found as expected that E_g decreases linearly as E_0 increases. This is also theoretically understood [34]. E_0 depends on dye molecule while E_1 depends on chelate Cu(N-R-salim)$_2$.

Conclusion

The FTIR spectra of Cu(N-R-salim)$_2$ where R = H, CH_3, C_2H_5, and C_6H_5 hydrogen bonded with six highly polarizable dyes are studied and analyzed in the present work. Nature of transitions is fitted, which are usually found to be indirect transitions. The number of phonon bands vs. band gap graphs are plotted, which show rectilinear behavior for R = H, CH_3 and C_2H_5, but for R = C_6H_5 these graphs show deviation from a linear correlation. Exciton-phonon coupling decreases as the number of phonon band increases; thus band gap decreases with increase in exciton-phonon coupling.

References

[1] Oza, A. T. (1989). *Solid State Commun.*, *71*, 1005.
[2] Patel, K. D., & Oza, A. T. (1997). *Ind. J. Phys.*, *71B*, 161.
[3] Patel, R. G., & Oza, A. T. (2000). *Ind. J. Phys.*, *74B*, 31.
[4] Patel, M., Patel, S. G., Vaidya, R., & Oza, A. T. (2003). *Ind. J. Phys.*, *77B*, 199.
[5] Patel, R. G., Solanki, G. H., Prajapati, S. M., & Oza, A. T. (2004). *Ind. J. Phys.*, *78A*, 471.
[6] Oza, A. T., Patel, S. G., Patel, R. G., Prajapati, S. M., & Vaidya, R. (2005). *Thin Solid Films*, *477*, 153.
[7] Patel, M., Patel, S. G., Dave, M., & Oza, A. T. (2004). *Ind. J. Pure Appl. Phys.*, *42*, 79.
[8] Trivedi, P., Patel, A., Patel, R. G., Patel, V. A., & Oza, A. T. (2005). *Ind. J. Pure Appl. Phys.*, *43*, 335.
[9] Prajapati, J. H., Patel, S. G., & Oza, A. T. (2004). *Ind. J. Pure Appl. Phys.*, *42*, 572.
[10] Prajapati, J. H., Patel, S. G., & Oza, A. T. (2004). *Ind. J. Phys.*, *78*, 1365.
[11] Patel, M., Dave, M., Patel, K. R., & Oza, A. T. (2006). *Prajna-SPU Res. J.*, *14*, 117.
[12] Patel, A., Trivedi, P., & Oza, A. T. (2006). *Ind. J. Phys.*, *80*, 1201.

[13] Prajapati, J., Patel, K. R., Dave, M. S., Vaidya, R., Patel, S. G., & Oza, A. T. (2007). *J. Ind. Chem. Soc.*, *84*, 750.
[14] Patel, A. N., & Oza, A. T. (2008). *Mol. Cryst. Liq. Cryst.*, *482*, 117.
[15] Agravat, S., Jain, V., & Oza, A. T. (2008). *Ind. J. Chem.*, *47A*, 341.
[16] Oza, A. T., Solanki, G. K., Amin, A., & Trivedi, P. (2008). *Ind. J. Phys.*, *82*, 1513.
[17] Solanki, G. K., Patel, M., & Oza, A. T. (2008). *Prajan-SPU Res. J.*, *16*, 150.
[18] Oza, A. T., Solanki, G. K., Ray, A., & Amin, A. (2010). *Ind. J. Phys.*, *84*, 1529.
[19] Padhiyar, A., Patel, A. J., & Oza, A. T. In communication.
[20] Parmar, H., & Oza, A. T. In communication.
[21] Pandhiyar, A., Patel, A. J., & Oza, A. T. (2007). *J. Phys. Condens. Matter*, *19*, 486214.
[22] Prajapti, S. M., Oza, A. T., Talpada, N., & Patel, R. G. (1999). *Prajna-SPU Res. J.*, *9*, 51.
[23] Pankove, J. I. (1970). *Optical Processes in Semi-Conductors*, Prentice-Hall Inc.: Englewood Cliffs, NJ.
[24] Gersherzon, M., Thomas, D. G., & Dietz, R. E. (1962). In: *Proceedings of the International Conference on Semiconductor Physics Exeter*, Institute of Physics and Physical Society: London.
[25] Dean, P. J., & Thomas, D. G. (1966). *Phys. Rev.*, *150*, 690.
[26] Bouma, T., Scholten, A. J., Zondag, H. A., Luijendijk, T. J., & Dijkhuis, J. I. (1994). *Phys. Rev. B*, *49*, 1720.
[27] Hrokhmal, A. P. (2003). *Semiconductors*, *37*, 249.
[28] Salvador, M. R., Graham, M. G., & Scholes, G. D. (2006). *J. Chem. Phys.*, *125*, 184709.
[29] Vogelsang, H., Stolz, H., & Von der Osten, W. (1996). *J. Luminiscence*, *70*, 414.
[30] Masumoto, Y., Kawamura, T., Ohzeki, T., & Urabe, S. (1992). *Phys. Rev. B*, *46*, 1827.
[31] Mendelsberg, R. J., Allen, M. W., Durbin, S. M., & Reeves, R. J. (2011). *Phys. Rev. B*, *83*, 205202.
[32] Kanemitus, Y., Masuda, K., Yanaka, H., Ando, M., Kushida, T., Min, K. S., & Atwater H. A. (2002). *Phys. Stat. Sol. (a)*, *190*, 529.
[33] Perebeinos, V., Tersoff, J., & Avouris, P. (2005). *Phys. Rev. Lett.*, *94*, 27402.
[34] Grein, C. H., & John, S. (1989). *Phys. Rev. B*, *39*, 1140.